

Dry three-dimensional bubbles: growth-rate, scaling state and correlations

Stéphane Jurine^a, Simon Cox^{b, 1}, François Graner^{a,*}

^a *Spectrométrie Physique, UMR 5588 CNRS, Université Joseph Fourier, 140 rue de la Physique, BP 87, 38402 Saint Martin d'Hères Cedex, France*

^b *Department of Physics, Trinity College, Dublin 2, Ireland*

Received 1 October 2004; accepted 21 January 2005

Available online 26 February 2005

Abstract

The energy and shape of three-dimensional clusters of equal-volume bubbles packed around a central bubble are calculated. The resulting surface areas and bubble pressures provide an improvement upon existing growth laws for three-dimensional bubble clusters. Since a bubble's growth-rate depends mostly on its number of faces, simulations of coarsening can be accelerated by considering bubble topology rather than detailed geometry. The coarsening-induced relaxation of a disordered foam towards a scaling state, in which the normalised bubble volume and face-number distributions remain invariant, can thus be characterised.

© 2004 Elsevier B.V. All rights reserved.

PACS: 82.70.Rr; 83.80.Iz

Keywords: Foam; Clusters; Bubbles; Coarsening; Surface Evolver

1. Introduction

1.1. Goals of this paper

Recent progress in experiments, simulations, and theory have motivated us to address the main open questions in the coarsening of dry foams: (i) what is the exact growth law for an individual bubble? (ii) is it sensitive to detailed bubble topology and deviation from isotropy? (iii) how do the distributions of bubble volumes (normalised, throughout this paper, by the average volume at a given time) and number of faces vary with time? (iv) do these distributions converge towards an asymptotic state? (v) is this asymptotic state always the (previously identified) scaling state, that is, is it robustly independent of initial conditions, details

of the growth-rates of individual bubbles, and mechanical equilibration? (vi) what are the correlations between a bubble's volume, its number of faces, and the properties of its neighbours? The present paper summarises results and partial answers which we have or will present in detail elsewhere [1,2].

1.2. Current state of knowledge

A dry foam in three dimensions (3D) reaches mechanical equilibrium on time-scales of the order of 10^{-6} – 10^{-3} s. This equilibrium state then further relaxes through gas diffusion; here we do not consider drainage and film breakage, which cause deviations from equilibrium. Typical coarsening time-scales are of the order of 10 – 10^3 s [3]; hence at each point in time the foam is in mechanical equilibrium. Studies of foam coarsening require the accurate calculation of the bubbles' surface areas, and also pressure differences between bubbles (Eq. (1)), which in turn depend on the bubble geometry at equilibrium. Analytical and experimental results are notoriously difficult to obtain, as are simulations, which are

* Corresponding author. Fax: +33 4 76 63 54 95.

E-mail addresses: foams@aber.ac.uk (S. Cox), graner@ujf-grenoble.fr (F. Graner).

¹ Present address: University of Wales Aberystwyth, Institute for Mathematical and Physical Sciences, Aberystwyth SY23 3BZ, UK.

also time consuming due to the large difference between these time-scales [4]. We can summarise our current level of understanding as follows.

In two-dimensions (2D), von Neumann [5] showed analytically that the growth-rate of a bubble (of area A) is directly proportional to its number of sides, n : $dA/dt \propto (n - 6)$. That is, it depends upon bubble topology only, irrespective of the precise geometry. This result, confirmed experimentally [6,7], considerably simplified studies of 2D coarsening, enabling irrelevant geometrical details to be ignored. Experiments, simulations and analysis finally agreed that the average size $\langle A(t) \rangle$ increases linearly with time [8] and that a “scaling state” exists, in which the distributions of normalised bubble sizes ($A/\langle A(t) \rangle$) and face-number remain invariant during coarsening [9]. See [8] for a more detailed review of 2D coarsening.

In 3D, the growth-rate of a bubble of volume V is a sum over its i faces [10], each with surface area S_i , pressure difference Δp_i and mean curvature H_i

$$G = \frac{3}{2D_{\text{eff}}} \frac{dV^{2/3}}{dt} = -\frac{1}{2} \sum_i \frac{\Delta p_i S_i}{\gamma V^{1/3}} = -\frac{1}{V^{1/3}} \int_i H_i dS_i. \quad (1)$$

We use here the convention that the mean curvature is $H_i = \frac{1}{2}(1/R_{i1} + 1/R_{i2})$ [1,11,12], where R_{i1} and R_{i2} are the principal radii of curvature. Thus some expressions for G below differ from those in articles which use a convention without the factor of 1/2 [10]. With the present convention, the pressure difference Δp_i is *twice* the mean curvature H (multiplied by the tension γ). We assume that the effective diffusion coefficient D_{eff} of the gas across the bubble walls, and the wall tension $\gamma = 2\gamma_{\text{air-water}}$, are constant and are irrelevant to what follows (we take $D_{\text{eff}} = \gamma = 1$ without loss of generality). As in 2D, where the area rather than the perimeter of each bubble is the significant quantity, here only the volume matters, not the surface area. Does the 3D growth law depend only on the bubble topology? In fact it does not; but *if* the dispersion about such a law was found to be small, expressing the average growth-rate of F -faced bubbles as a function of F only, $G \approx G(F)$, might be convenient.

The growth of *grains* in crystals is similar to foam coarsening, but without the time-scale separation, so that grains do not equilibrate [8]. Grains are thus simpler to simulate than foams. Mullins [13] assumed that G was approximately a function of the grain face number F only. He assumed that grains are regular polyhedra and their faces only weakly curved. He calculated their geometrical properties by approximating each face as a pentagon obeying Plateau’s rules, assuming that his results do not depend much on the detailed topology (as was later checked in 2D [14] and in 3D [12]). He then predicted analytically an expression for G versus F (which changes sign for $F \approx 13.3$):

$$G_{\text{Mull}}(F) = \frac{1}{2} \left(\frac{3}{4\pi} \right)^{1/3} G_1(F) G_2(F), \quad (2)$$

where

$$G_1(F) = \frac{\pi}{3} - 2 \arctan \left[1.86 \frac{(F-1)^{1/2}}{F-2} \right],$$

and

$$G_2(F) = 5.35 F^{2/3} \left[\frac{F-2}{2(F-1)^{1/2}} - \frac{3}{8} G_1(F) \right]^{-1/3}.$$

We have introduced a factor of 1/2, to relate the driving force for grain growth to the mean-curvature of soap films. Mullins checked, using an experimental distribution $\mathcal{P}(r)$ of grain sizes and a conditional distribution $\mathcal{P}(F|r)$ of faces, that to a very good approximation G_{Mull} satisfies the total volume conservation condition:

$$\frac{\langle r \rangle^2}{\pi \langle r^6 \rangle} \int dr \mathcal{P}(r) \sum_F \mathcal{P}(F|r) G(F) = 0. \quad (3)$$

Finally he showed that, if the grains reached a scaling state, $d\langle r^2 \rangle/dt = \text{const}$.

Grain growth simulations suggested that such a scaling state does exist [15,16]. Glazier [10] checked that the dependence of G was mostly on topology, using simulations with 4000 grains; his figure 1a is apparently compatible with Mullins’ prediction but, unaware of it, Glazier suggested that the deviation from linearity might be due to simulation artifacts and presented in his figure 1b a linear law similar to the 2D one. Wakai et al. confirmed numerically Mullins’ expression for $G(F)$, in a detailed paper [17] which the foam community probably does not quote enough [4]. With a quick scheme to perform wall movement and T1s without equilibration, they used the Surface Evolver [18] to simulate a collection of one thousand grains. They found that this growth-rate, as well as correlations (see below), was the same during the coarsening, and hence did not depend on the particular grain distribution. After coarsening, the grain distribution *apparently* became time-independent (evidence is alluded to, but not given), indicating that it had reached a scaling state with average face number $\langle F \rangle = 13.5$ (decreasing from 14 in the initial condition) and apparently compatible with Mullins’ $d\langle r^2 \rangle/dt = \text{const}$. The existence and properties of a scaling state for foams may soon be clarified by recent experiments, such as those using X-ray tomography [19], with which thousands of 3D bubbles can be investigated over long periods of time.

Knowing the growth-rate (determined at equilibrium, Eq. (1)) is necessary but not sufficient to understand coarsening, i.e. the statistical evolution of bubble distributions. Almeida et al. took another point of view and, refining a maximal entropy suggestion of Rivier [20], studied foams disordered enough to maximise their free energy, through competition between entropy increase under shuffling and energy minimisation due to surface tension. Using statistical arguments, they predicted the distribution of sizes and face numbers first

in 2D [21], in agreement with experiments [6,7], then in 3D [22], apparently in good agreement with the simulation results of Wakai et al. [17].

The growth-rate of *bubbles* proved more difficult to investigate. Experimentally, observing enough 3D bubbles for a long enough time to extract significant statistics was a difficult challenge which involved years of careful work [23,24,4,25]. Hilgenfeldt et al. [26] used an elegant approximation to derive an analytical result for ideal bubbles, later supported by simulations of large foams [27,28] and realizable regular bubbles [11]:

$$G \approx G_{\text{Hilg}}(F) = \frac{3}{2^{1/3}} \left[(F-2) \tan\left(\frac{\pi}{n_F}\right) \right]^{2/3} \times \tan^{1/3}\left(\frac{\chi_F}{2}\right) \left(\frac{\pi}{3} - \chi_F\right), \quad (4)$$

where $\chi_F = 2 \tan^{-1} \sqrt{4 \sin^2(\pi/n_F) - 1}$ and $n_F = 6 - 12/F$ is the number of edges per face.

This result was recently improved [12], using Mullins' method [13] without the pentagonal-face approximation, to give an exact result for “isotropic Plateau polyhedra” (IPP); these are ideal bubbles with spherical-cap faces whose growth-rate is based upon an interpolation between the realizable, regular, bubble shapes: the tetrahedron, cube and dodecahedron. This growth-rate is:

$$G_{\text{IPP}}(F) = 72^{1/3} \left(F n_F \right)^{2/3} \frac{\sin^{-1}(1/\sqrt{3}R) + \cos^{-1}(1/3) - (2\pi/n_F)}{\left(2\sqrt{2} + (48\pi/n_F) - 57 \cos^{-1}(1/3) + 33y - \tan(y) \right)^{1/3}} \quad (5)$$

where $R = \frac{3}{2} \left(\sqrt{8 \sin^2(\pi/n_F) - 2} - \cos(\pi/n_F) \right)^{-1}$ and $\sin(y) = \frac{2}{\sqrt{3}} \cos(\pi/n_F)$. Both G_{IPP} and G_{Hilg} change sign for $F \approx 13.4$ and, as we shall show below, are close to Mullins' expression [13], suggesting that bubbles and grains have similar growth-rates.

1.3. Outline of this paper

Our approach is based upon the study of finite clusters of bubbles. In small clusters, we get detailed and accurate measures of the shape and geometrical properties of freely equilibrated bubbles. We can thus precisely determine the individual growth laws and effects of bubble regularity. We then use large periodic clusters to collect statistics necessary for histograms and correlations. We present here our preliminary results for clusters of 512 bubbles, for which the statistics should be considered as indicative only, rather than comprehensive. Since a bubble's growth-rate mostly depends on its number of faces, which we know from our results for small clusters, we accelerate our coarsening simulations by considering only bubble topology rather than detailed geometry. We thus characterise the relaxation of a disordered foam towards an asymptotic regime for equilibrated bubbles which we identify with the scaling state (for grains and bubbles) found previously [17].

2. Small clusters

2.1. Methods

For further details of small clusters see [1]. We use the Surface Evolver [18] to take a central bubble of volume V_c and surround it with F bubbles, each with the same volume V , as shown in Fig. 1. We arrange the neighbours as regularly as possible around the central bubble. Hence, for all values of F

where regularity is not realizable, the central bubble is as regular as possible (we call such bubbles “quasi-regular”). We study simple ratios of V_c/V to explore F from 4 to 60, and measure the surface area S , edge-length L and growth-rate G_{sim} of each central bubble, all accurate to at least four decimal places of accuracy. We use an Evolver mesh of quadratically curved triangular faces with three-fold refinement.

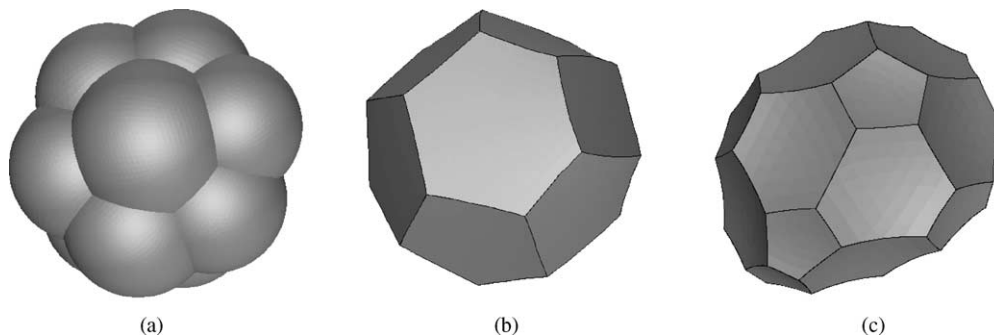


Fig. 1. Examples of the clusters we consider, with all bubble volumes equal: (a) cluster of $F = 13$ outer bubbles (that is, a total of $F + 1 = 14$ bubbles) still attached; (b) the quasi-regular central bubble, drawn to a different scale, with $F = 13$ faces (this is a Matzke cell [27] with one square, 10 pentagonal and two hexagonal faces); (c) a central bubble with $F = 26$ faces (all pentagonal or hexagonal) — note its departure from approximate sphericity.

2.2. Correlation between number of faces and shape

The shape factor $S/V^{2/3}$ (normalized surface area) characterises the deviation of a bubble from sphericity. It is almost constant for our quasi-regular bubbles, as proved in 2D [14] and 3D [12]. There is a small, non-monotonic fluctuation, so that in general the value of S decreases slightly as the volume ratio increases.

For each value of V_c/V , the physically realizable values of F are limited. Within the possible F , the $S(F)$ curves admit an optimum: a value of F which minimises the bubble area. These optimal F values increase with V_c/V [1].

The dimensionless edge-length $L/V^{1/3}$ of each bubble lies close to a line $L/V^{1/3} \propto \sqrt{F}$ [11] with no drastic dependence on V_c/V . The square-root approximation becomes slightly worse as the bubbles become larger and gain more faces, with the maximum deviation occurring at higher F for increasing V_c/V .

We can express both the volume and surface area of an F -faced bubble in terms of the average length \hat{l} of the edges around it: V/\hat{l}^3 and S/\hat{l}^2 . These quantities, which are useful in the study of foam drainage [3,29], both increase strongly with the number of faces F and are insensitive to the size of the neighbouring bubbles [1].

2.3. Correlation between number of faces and growth-rate

We calculate the instantaneous growth-rate G_{sim} of each bubble through the formula (1), shown in Fig. 2, except at (for us unobtainable) small F where the results of Cox and Fortes [11] for $F = 2$ and 3 are useful.

For $F \geq 12$ our data suggest that G_{Hilg} is a better approximation to the average growth-rate than G_{Mull} and G_{IPP} . The dispersion around this average due to differences in the volumes of neighbouring bubbles is less than 1%, emphasising the quality of the approximation that bubble topology dictates the growth-rate.

In a coarsening foam, bubbles with low F are important, because it is these bubbles that disappear. For $F < 12$, our data for quasi-regular bubbles are significantly (up to 10%) larger than the analytical prediction of G_{Hilg} . Our data are closely clustered; for small F they lie within 0.1% of the prediction of G_{Mull} and G_{IPP} . For $F < 12$, both Eqs. (2) and G_{IPP} , and our data, are thus probably much more accurate than G_{Hilg} , since the approximation should gradually lose its validity at low F [26]. Table 1 lists the growth-rates for quasi-regular bubbles with $F \leq 12$, averaged over all simulations.

2.4. Correlation between number of faces and volume

Real foams often have a distribution of bubble volumes, and their topology correlates with their geometry: larger bubbles tend to have more neighbours [30].

Table 1

The growth-rates, averaged over all simulations, $G_{\text{reg}}(F) = \langle G_{\text{sim}}(F) \rangle$ for quasi-regular bubbles with few faces, $F \leq 12$

F	$-G_{\text{reg}}(F)$
2	5.632
3	4.655
4	3.967
5	3.326
6	2.849
7	2.350
8	1.899
9	1.506
10	1.130
11	0.760
12	0.453

They agree closely with the expression for ideal bubbles, Eq. (5) [12] and show very little dispersion.

Such correlations appear in our study of individual bubbles, although we did not specifically include them. They are easy to explain qualitatively. Since each bubble has a surface area which grows like $V^{2/3}$, its faces have an average surface area going like $V^{2/3}/F$. Since neighbouring bubbles share a common face, they should have a similar value of $V^{2/3}/F$; thus bubbles with larger V tend to have larger F .

Such rough mean-field approximations cannot predict in detail the correlations [21] in actual foams. The simulations of Wakai et al. on grains [17] have confirmed more detailed predictions [22] and suggest that a large- F bubble has smaller- F neighbours (topological correlations), as in 2D (Aboav–Weaire laws) [3].

Hence simulations of individual bubbles cannot capture the essence of the physics, and we turn to large, periodic, clusters.

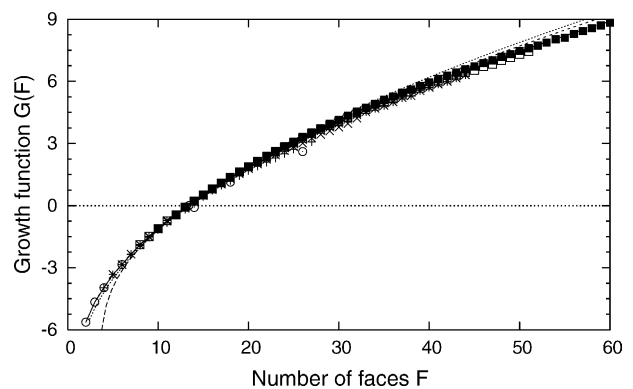


Fig. 2. The rate of change of volume of a bubble with F faces: the value $G_{\text{sim}}(F)$ calculated from our simulations of small clusters using Eq. (1), for volume ratios of $V_c/V = \frac{1}{2}$ (+), 1 (x), 2 (*), 3 (□) and 5 (■). The data for bubbles with constant curvature (⊙) [11], rather than fixed volume, is more scattered, but useful for low F . Also shown are $G_{\text{reg}}(F)$ (solid line), $G_{\text{Mull}}(F)$ (short dashes), $G_{\text{IPP}}(F)$ (dotted line) and $G_{\text{Hilg}}(F)$ (long dashes). The latter deviates from the data at small F , while the IPP and Mullins' formula deviate from the data at large F .

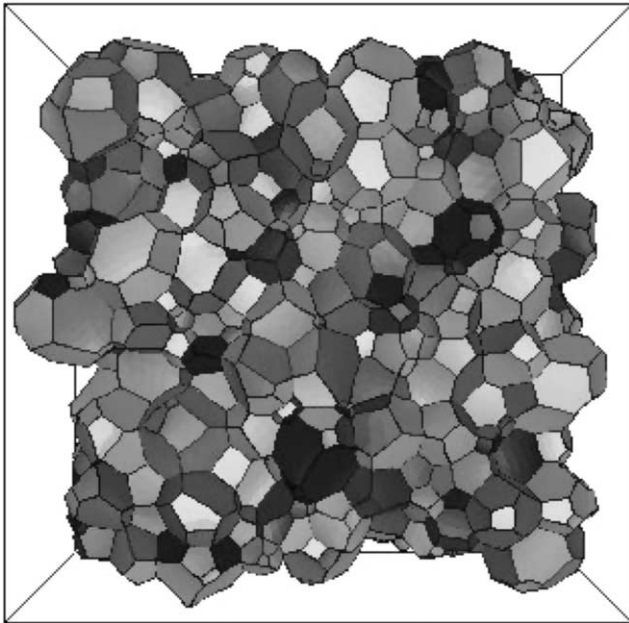


Fig. 3. An example of a periodic cluster after 10 coarsening steps, which have taken the number of bubbles from 512 to 502.

3. Large clusters

3.1. Methods

For further details of large clusters see [2]. We take a periodic foam with between 128 and 512 bubbles and a large initial volume distribution (Fig. 3), obtained from a Voronoi construction using Sullivan’s VCS software [31]. This initial condition is random and locally well-relaxed, like a real foam, which is at a local mechanical equilibrium. It is not at a global equilibrium, and possible residual stresses are not relaxed [32] (this is acceptable here, since we investigate only the topology, in contrast to the detailed and carefully relaxed simulations of Kraynik et al. [27,28]).

To coarsen a large cluster of bubbles, at each time step we count the number of faces F of a bubble and estimate G from our small cluster calculations, using Table 1 up to $F < 12$, and Eq. (4) for $F \geq 12$. That is, we approximate G by $G_{\text{reg}}(F)$ defined as:

$$\begin{aligned} G_{\text{reg}}(F) &= \langle G_{\text{sim}}(F) \rangle_F, & (F < 12), \\ G_{\text{reg}}(F) &= G_{\text{Hilg}}(F), & (F \geq 12). \end{aligned} \quad (6)$$

We then adjust the target volume of each bubble according to $V^{2/3}(t + dt) = V^{2/3}(t) + (2/3) dt G_{\text{reg}}(F)$ and partially equilibrate, by alternating geometrical relaxations which decrease the surface area (using the “gradient descent” iteration command of the Surface Evolver [18]) with topological relaxations of unstable vertices and edges (“popping” commands). A time-step ends when no five-fold vertices nor four-fold edges remain, and all eigenvalues of the Hessian of energy are positive. We then re-count the number of faces and iterate.

Even within these simplifications, the book-keeping of T1s is far from trivial, as is the adaptive triangulation of bubble faces with a small cut-off [2]. Note that, in contrast to the small cluster calculations, we use a Surface Evolver mesh of unrefined plane (linear) triangular faces.

Since we do not completely relax the geometry (curvature, pressures) in the intervals between T1s, we know that we will have omitted some T1s (it would take much longer to compute all T1s [33]). However, since we specifically want to test the robustness of the scaling state, a more detailed equilibration is not necessary.

Our first simulations used a time step small enough to produce, on average, not more than a single T1 per time step. We then accelerated our simulations by increasing the time step to produce exactly one T2 per time step (using $G(F)$ to predict the time of the next T2), and therefore multiple T1s (and hence many Surface Evolver iterations), and checked that the results presented below do not change.

3.2. Correlation between number of faces and shape

Volume, surface area and edge length correlate with the number of faces (Fig. 4), generalising the 2D empirical relations between side number and area (Lewis Law) or perimeter (Feltham). We observe that these correlations are not specific to the scaling state, and do not seem to depend on the volume distribution, compatible with Wakai’s results [17]. None of these correlations is strictly linear; the less curved is certainly that of edge-length L versus number of faces F (Fig. 4, bottom right). Hence, if an analytical study of foam disorder, such as that of Almeida et al. [22], must assume a linear correlation between F and another quantity, the best empirical approximation would be to use $F(L)$.

3.3. Correlations between neighbouring bubbles

The sizes of neighbouring bubbles anti-correlate: a bubble larger than average, with large F , has neighbours smaller than average, with small F . This Aboav–Weaire law [34] has been well characterised in 2D. In 3D, again, there are grain growth simulations [17].

If a bubble has F faces and the average number of faces of its neighbours is $F_{\text{neighbours}}$, we observe that at each time, the correlation between $F_{\text{neighbours}} \times F$ and F is a straight line (Fig. 5, left). We would thus like to check whether we can generalise the 2D formula [34] by writing:

$$F \times F_{\text{neighbours}} = (\langle F \rangle - a)F + (a\langle F \rangle + \mu_2^F), \quad (7)$$

where $\langle F \rangle$ is the average (usually close to 13 or 14) and μ_2^F is the second moment of the foam’s F -distribution; a is an unknown parameter. On the right hand side, the first parenthesised term is the slope of the fit and the second term is the linear intercept. Measuring both leads to two independent measurements of a ; both are equal within measurement errors (Fig. 5, right).

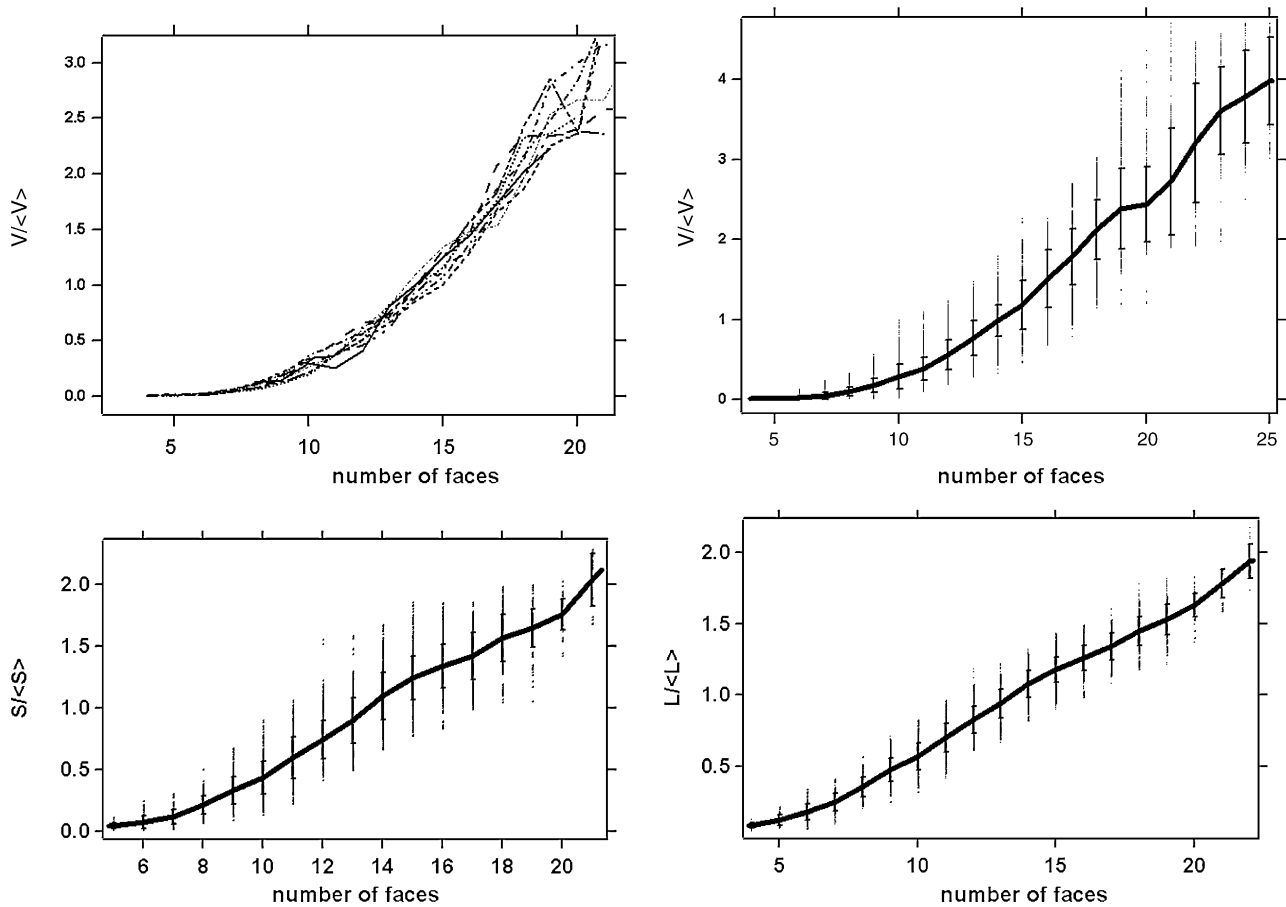


Fig. 4. Size-topology correlations in 3D, generalising the 2D “Lewis” and “Feltham” relations. (Top left) The relation between bubble volume and number of faces, here plotted at successive times, does not significantly evolve during coarsening. The non-smooth nature of the curves, and those following, probably indicates that our statistics are insufficient to draw strong conclusions. (Top right) To improve the statistics, we superimpose the successive curves of the top left figure (dots = individual bubbles’ values; solid line = average for each value of F ; bars = standard deviation for each value of F). Bubble volume correlates with the number of faces, but this correlation is not linear. (Bottom left) Same plot for the dimensionless surface area of each bubble. (Bottom right) Same plot for the dimensionless edge-length.

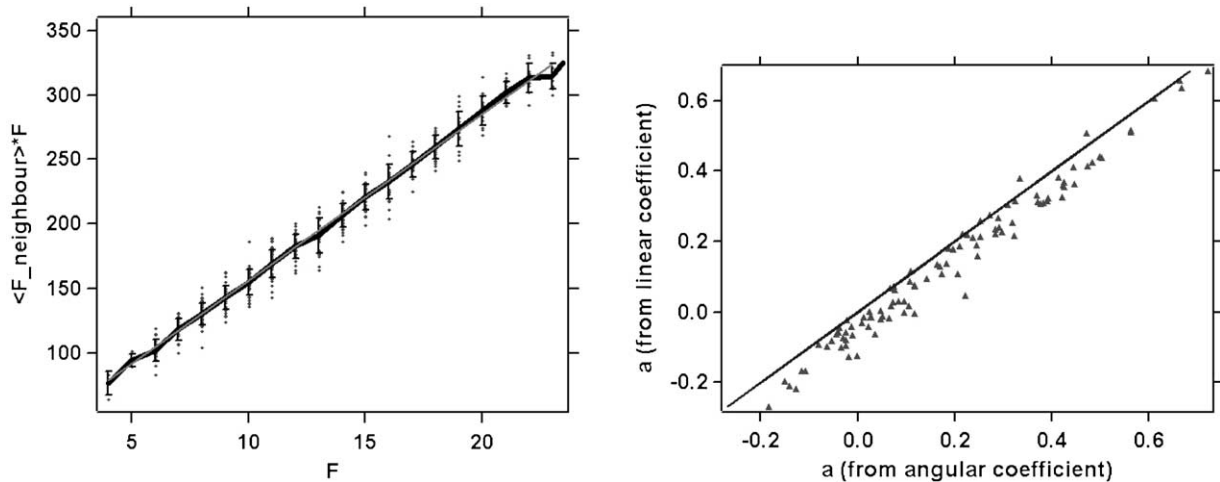


Fig. 5. 3D Abcav–Weaire law. (Left) Correlation between the number of faces of a bubble and of its neighbours for a coarsening foam at a given time; dots = individual bubble values; solid line = average for each value of F ; bars = standard deviation for each value of F ; thin grey line = linear fit. (Right) Two different measures (see text) of the unknown parameter a from the linear fit by assuming Eq. (7); one is plotted vs. the other for the same foam at each time-step. The solid line is the diagonal ($y = x$).

A third method, suggested by Kraynik [33], measures a without requiring any fit: Eq. (7) implies

$$a = \langle F \rangle - \frac{1}{\mu_2^F} [\langle F^2 (F_{\text{neighbours}} - \langle F \rangle) \rangle]. \quad (8)$$

Thus we obtain a from a direct measure of the difference between each bubble's number of faces and that of its neighbours; the results (not shown) are similar to those given above.

3.4. Growth-rate of individual bubbles

With small clusters (Section 2.3), we have precisely determined the growth-rate $G_{\text{reg}}(F)$ for regular bubbles; we have also estimated the dispersion of the actual G around $G_{\text{reg}}(F)$, for $F \geq 12$. With large clusters, we can increase our understanding of this dispersion.

The Surface Evolver provides us with each bubble's pressure (see however the *caveat* below) and each face's surface area. We can determine each bubble's G from Eq. (1), and compare it with the value $G_{\text{reg}}(F)$ determined for a regular bubble with the same number of faces. Two main results emerge (Fig. 6, left).

First, the growth-rate does not vary much with bubble shape, confirming earlier findings and explaining why Mullins' and Hilgenfeldt's expressions for symmetric grains and bubbles were already good approximations to actual bubbles [13,26].

Second, actual bubbles with F faces almost all grow (with a very few exceptions, visible as dots above the dashed line for $F = 14$ or 20) more slowly than a regular bubble with F faces. The average growth-rate $\langle G \rangle_F$ of all bubbles with F

faces constitutes a curve which parallels the curve for ideal bubbles (a trend already apparent, but not quantified, in [26]); the shift, shown in Fig. 6, left, is roughly equal to one face ($\delta F \approx 1$). To simulate the growth of an F -faced bubble, we could therefore use the approximation:

$$G \approx \langle G \rangle_F \approx G_{\text{reg}}(F - 1). \quad (9)$$

Bubbles with the same face number F are not all alike. A bubble has a detailed topology, quantified by the distribution of its number n of sides per face (for instance, a Matzke cell has 1 four-sided, 10 five-sided and 2 six-sided faces, Fig. 1b). On average $\langle n \rangle = 6 - 12/F$, due to Euler's theorem [3], so all bubbles with the same F have the same $\langle n \rangle$. The standard deviation δn of the distribution of the number of sides of a bubble quantifies its topological disorder. This detailed topology changes the growth-rate: at fixed F , the growth-rate G tends to decrease with disorder δn (Fig. 6, right).

The values of pressure p that the Surface Evolver reports for unrelaxed structures are not reliable. We have checked the results above by thoroughly relaxing a cluster (at one instant in time) and comparing the results (data not shown). We find that, at least for foam statistics, our simulations capture the essence of the physics. Kraynik [12,33], using carefully refined simulations, recently confirmed our findings: the growth-rate of regular F -faced bubbles is statistically an upper bound for the growth-rate of other F -faced bubbles, but some bubbles violate it.

Finally, note that G might have a small systematic dependence on statistical parameters of the structure [35], for instance the second moment μ_2^F of the foam's F -distribution.

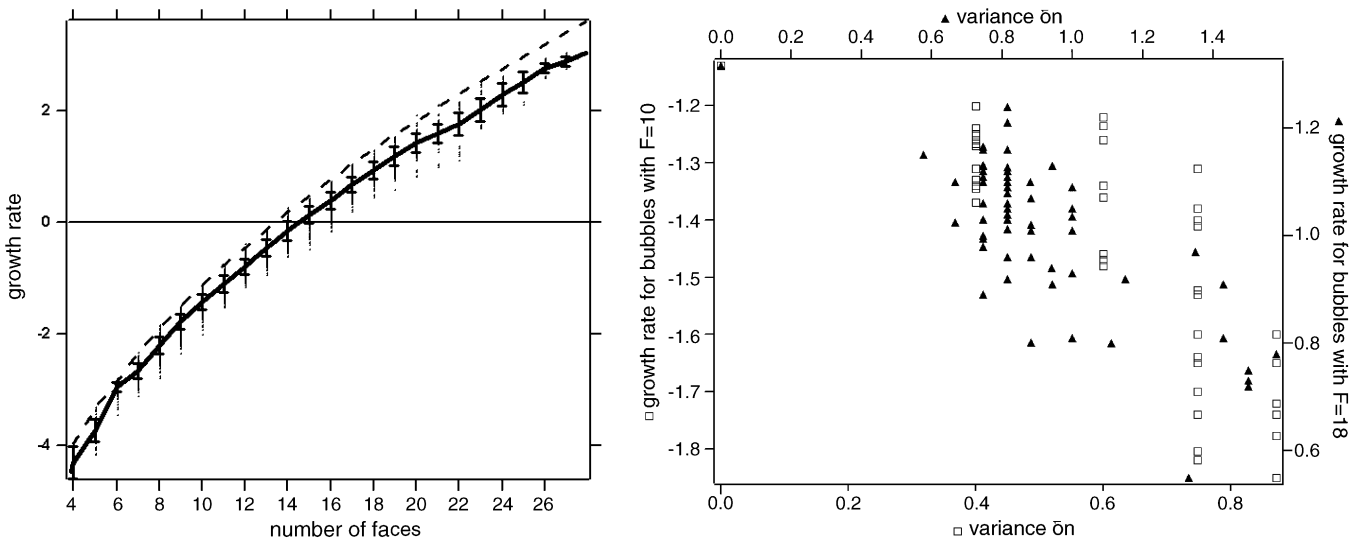


Fig. 6. Correction due to bubble shape irregularity. (Left) Actual bubbles with F faces have a growth-rate G (dots = individual bubbles' values of G ; thick solid line = average $\langle G \rangle_F$ for each value of F ; bars = standard deviation of G for each value of F which is almost always lower than that of a regular bubble with F faces ($G_{\text{reg}}(F)$, dashes). Its average $\langle G \rangle_F$ is that of a regular bubble with $\approx F - 1$ faces. (Right) The difference from a regular bubble's $G_{\text{reg}}(F)$ increases with the bubble's topological disorder, quantified by the variance δn in its number of sides per face. We plot data for various F -faced bubbles for two examples: $F = 10$ (open squares, left and bottom axes) and $F = 18$ (closed triangles, right and top axes), rescaling so that simulated quasi-regular bubbles [1] (symbolically plotted as zero variance) with $F = 10$ (2 four-sided and 8 five-sided faces) and $F = 18$ (12 five-sided and 6 six-sided faces) coincide.

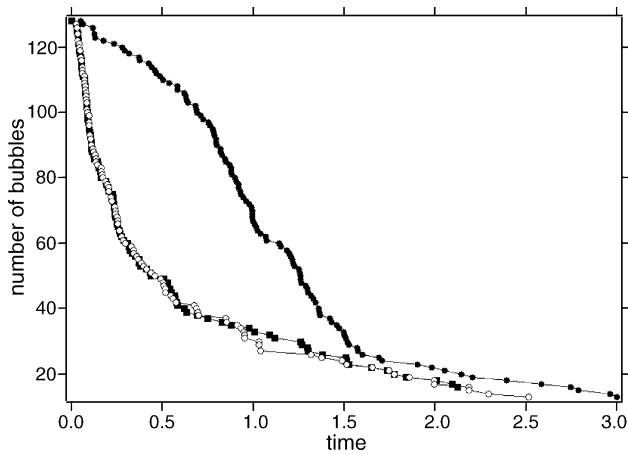


Fig. 7. The number of bubbles vs. time. Comparison between 128-bubble clusters with an initially exponential volume distribution (using $G_{\text{reg}}(F)$, closed squares, or G , open circles) and an initially peaked distribution (using $G_{\text{reg}}(F)$, closed circles). Time units correspond to D_{eff} and the total foam volume NV is an arbitrary constant (Eq. (1)).

3.5. Scaling state

Our simulations determine (Fig. 7) the number N of bubbles versus time (or equivalently the average volume $\langle V(t) \rangle$, since the total foam volume is constant), and the statistical properties of the bubble distributions during coarsening.

The distributions of normalised bubble volumes $V/\langle V(t) \rangle$ and numbers of faces F relax towards an asymptotic state, similar to (or at least compatible with) what grain growth simulations found to be a scaling state [15,17]. The present relaxation is robust under the following perturbations.

First, if we replace the growth-rate of regular bubbles $G_{\text{reg}}(F)$ (used here to speed up simulations, since it requires only the topology) by each bubble's growth-rate G (based on both topology and geometry, Eq. (1), even though the foam is not fully equilibrated), we obtain curves $N(t)$, shown in Fig. 7, which are indistinguishable, except for two T1s involving a few bubbles around time $t = 1.0$. This validation, performed with 128 bubbles, allows us to use only the quickest method to simulate 512 bubbles.

Second, starting the simulation from an initial volume distribution which differs greatly from the final one (e.g. an initially peaked distribution) leads to the same final state, albeit with a time lag corresponding to the duration of the transient regime (see Fig. 8).

4. Conclusions

The structure of a foam in equilibrium minimises its (free) energy, which is the product of (i) two characteristic quantities (surface tension and average surface area) and (ii) some function of shape only. The structure changes due to coarsening (in the absence of drainage and film breakage). The coarsening rate is the product of a diffusion constant (which

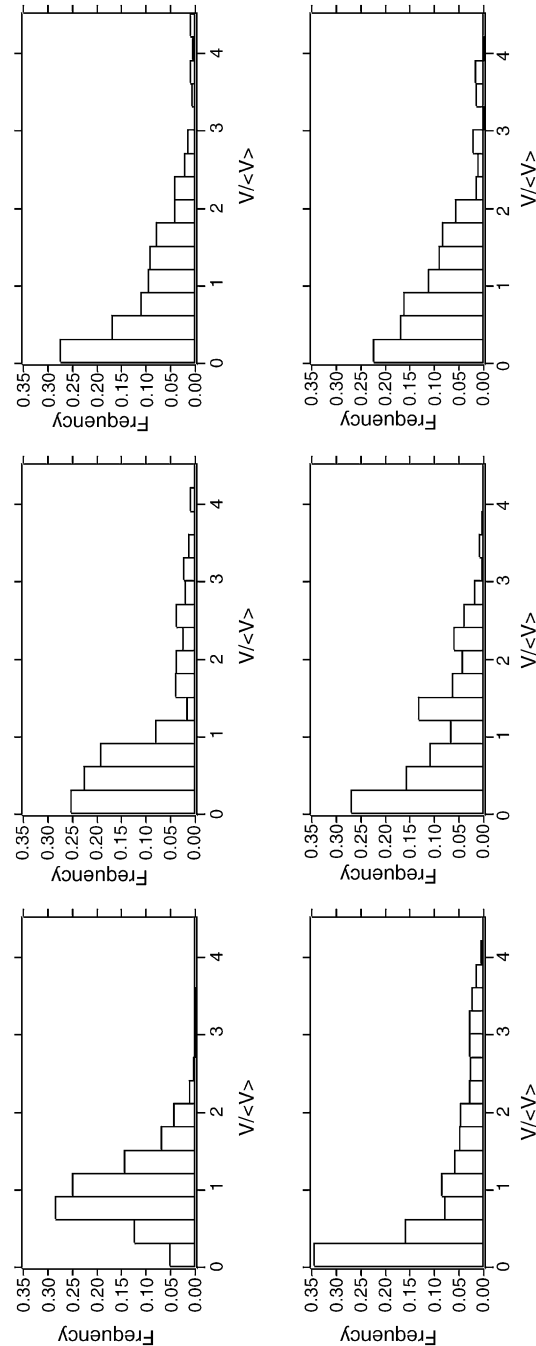


Fig. 8. Evolution of bubble volume distributions, starting from an initially exponential (upper row) or an initially peaked distribution (lower row). Each plot lumps the distributions for a given cluster at 10 successive time steps, starting at times 0 (left), 1 (centre) and 2 (right).

depends on the material parameters, including chemical composition), that sets the characteristic time scale, and a function only of geometry.

Using the Surface Evolver, we have studied both finite and periodic clusters of bubbles to obtain information about the structure of three-dimensional foam, the 3D coarsening law and scaling state. This approach allows us to accurately determinate the growth law for regular bubbles, in close agreement with the predictions of Hilgenfeldt et al. [12] and Mullins [13] for bubbles with fewer than 12 faces, and with the approximation of Hilgenfeldt et al. [26] for bubbles with 12 or more faces. In 3D, bubbles are close to regular (as in 2D), and their growth-rates close to those of regular bubbles.

We have determined corrections due to the irregularity of actual bubbles. The statistical properties of disordered foams are robust with respect to approximations: for instance, we retain the essence of the physics if we replace the bubbles' growth-rate by an average which depends only on the number of faces. Conversely, to measure detailed bubble properties, we suggest that the best-controlled approximation uses the exact result for regular bubbles with one less face. For fixed face number, the growth-rate tends to decrease with increasing topological disorder.

We have also obtained the *optimal* bubble shapes and surface areas for given bubble volumes, correlations between face numbers and geometrical properties (including “Lewis-like” relations: a large bubble has many faces) and with the neighbours' number of faces (3D Aboav–Weaire relations: a large bubble has small neighbours). We report other results elsewhere (see [1]): limiting possible values for the number of faces (with above- or below-average stability for certain values), “kissing” problems in 2D and in 3D (we observe that a maximum of 12 bubbles in 2D, and 32 bubbles in 3D, can pack around a central one).

Finally, we have obtained greater insight into how foams coarsen. Fast approximate simulations still catch the essence of the physics, if we assume that each bubble's growth-rate comes mostly from its number of faces. The scaling state (if it is confirmed) appears to be similar for grain growth and foam coarsening, and to be robust with respect to initial conditions and method of simulation. Future work requires better statistics to confirm our preliminary findings.

Acknowledgements

We warmly thank K. Brakke for having distributed and maintained his Surface Evolver program, and A. Kraynik, S. Hilgenfeldt, J. Glazier and D. Weaire who helped us with

unpublished results and fruitful criticism. Financial support is gratefully acknowledged from the Ulysses France-Ireland exchange scheme.

References

- [1] S. Cox, F. Graner, Phys. Rev. E 69 (2004) 031409.
- [2] S. Jurine, S. Cox, F. Graner, in preparation, 2005.
- [3] D. Weaire, S. Hutzler, The Physics of Foams, Clarendon Press, Oxford, 1999.
- [4] J. Glazier, B. Prause, in: P. Zitha, J. Banhart, G. Verbist (Eds.), Foams, Emulsions and their Applications, MIT-Verlag, Bremen, 2000, pp. 120–127.
- [5] J. von Neumann, Metal Interfaces, American Society for Metals, Cleveland, 1952, pp. 108–110.
- [6] J. Glazier, J. Stavans, Phys. Rev. A 40 (1989) 7398.
- [7] J. Stavans, J. Glazier, Phys. Rev. Lett. 62 (1989) 1318.
- [8] J.A. Glazier, Cellular patterns, Ph.D. Thesis, University of Chicago, 1989, unpublished.
- [9] J. Stavans, Rep. Progr. Phys. 56 (1993) 733.
- [10] J. Glazier, Phys. Rev. Lett. 70 (1993) 2170.
- [11] S. Cox, M. Fortes, Phil. Mag. Lett. 83 (2003) 281.
- [12] S. Hilgenfeldt, A. Kraynik, D. Reinelt, J. Sullivan, Europhys. Lett. 67 (2004) 484.
- [13] W.W. Mullins, Acta Metall. 37 (1989) 2979.
- [14] F. Graner, Y. Jiang, E. Janiaud, C. Flament, Phys. Rev. E 63 (2001) 011402.
- [15] M.P. Anderson, G.S. Grest, D.J. Srolovitz, Phil. Mag. B 59 (1989) 293.
- [16] K. Fuchizaki, T. Kusaba, K. Kawasaki, Phil. Mag. B 71 (1995) 333; K. Fuchizaki, K. Kawasaki, Physica A 221 (1995) 202.
- [17] F. Wakai, N. Enomoto, H. Ogawa, Acta Mater. 48 (2000) 1297.
- [18] K. Brakke, Exp. Math. 1 (1992) 141.
- [19] I. Cantat, R. Delannay, J. Lambert, J.A. Glazier, G.L. Caer, A. Renault, S. Ruellan, F. Graner, S. Jurine, P. Cloetens, Study of the coarsening of a 3d foam by microtomography, Presentation at EuFoam, in this proceedings, 2005.
- [20] N. Rivier, Physica D 23 (1986) 129.
- [21] R.M.C. de Almeida, J.R. Iglesias, J. Phys. A 21 (1988) 3365; J.R. Iglesias, R.M.C. de Almeida, Phys. Rev. A 43 (1991) 121.
- [22] R.M.C. de Almeida, J.C.M. Mombach, Physica A 236 (1997) 268.
- [23] C. Gonatas, J. Leigh, A. Yodh, J. Glazier, B. Prause, Phys. Rev. Lett. 75 (1995) 573.
- [24] C. Monnereau, M. Vignes-Adler, Phys. Rev. Lett. 80 (1998) 5228.
- [25] B. Prause, J.A. Glazier, in: M. Ding, W.L. Ditto, L.M. Pecora, M.L. Spano (Eds.), Proceedings of the 5th Experimental Chaos Conference, World Scientific, Singapore, 2001, p. 427.
- [26] S. Hilgenfeldt, A. Kraynik, S. Koehler, H. Stone, Phys. Rev. Lett. 86 (2001) 2685.
- [27] A. Kraynik, D. Reinelt, F. van Swol, Phys. Rev. E 67 (2003) 031403.
- [28] A. Kraynik, D. Reinelt, F. van Swol, Phys. Rev. Lett. 93 (2004) 208301.
- [29] S. Hilgenfeldt, S. Koehler, H. Stone, Phys. Rev. Lett. 86 (2001) 4704.
- [30] D. Weaire, J. Glazier, Phil. Mag. Lett. 68 (1993) 363.
- [31] J. Sullivan, [http://torus.math.uiuc.edu/jms/software/\(1988\)](http://torus.math.uiuc.edu/jms/software/(1988)).
- [32] V. Labiausse, S. Cohen-Addad, R. Höhler, Presentation at EuFoam, in this proceedings, 2005.
- [33] A. Kraynik, private communication, 2004.
- [34] D. Weaire, Metallography 7 (1974) 157.
- [35] D. Weaire, private communication, 2004.